

2015

# Arrival of the Fukushima Radioactivity Plume in North American Continental Waters

John N. Smith

Robin M. Brown

*See next page for additional authors*

Follow this and additional works at: <https://digitalcommons.uri.edu/gsofacpubs>

Terms of Use

All rights reserved under copyright.

---

## Citation/Publisher Attribution

Smith, J. N., Brown, R. M., Williams, W. J., Robert, M., Nelson, R., Moran, S. B. (2014). Arrival of the Fukushima radioactivity plume in North American continental waters. *Proceedings of the National Academy of Sciences*, 112(5), 1310-1315. doi: 10.1073/pnas.1412814112

Available at: <https://doi.org/10.1073/pnas.1412814112>

This Article is brought to you for free and open access by the Graduate School of Oceanography at DigitalCommons@URI. It has been accepted for inclusion in Graduate School of Oceanography Faculty Publications by an authorized administrator of DigitalCommons@URI. For more information, please contact [digitalcommons@etal.uri.edu](mailto:digitalcommons@etal.uri.edu).

---

**Authors**

John N. Smith, Robin M. Brown, William J. Williams, Marie Robert, Richard Nelson, and S. Bradley Moran

# Arrival of the Fukushima radioactivity plume in North American continental waters

John N. Smith<sup>a,1</sup>, Robin M. Brown<sup>b</sup>, William J. Williams<sup>b</sup>, Marie Robert<sup>b</sup>, Richard Nelson<sup>a</sup>, and S. Bradley Moran<sup>c</sup>

<sup>a</sup>Bedford Institute of Oceanography, Fisheries and Oceans Canada, Dartmouth, NS, Canada B2Y 4A2; <sup>b</sup>Institute of Ocean Sciences, Fisheries and Oceans Canada, Sidney, BC, Canada V8L 4B2; and <sup>c</sup>Graduate School of Oceanography, University of Rhode Island, Narragansett, RI 02882-1197

Edited by David M. Karl, University of Hawaii, Honolulu, HI, and approved December 2, 2014 (received for review July 28, 2014)

**The large discharge of radioactivity into the northwest Pacific Ocean from the 2011 Fukushima Dai-ichi nuclear reactor accident has generated considerable concern about the spread of this material across the ocean to North America. We report here the first systematic study to our knowledge of the transport of the Fukushima marine radioactivity signal to the eastern North Pacific. Time series measurements of <sup>134</sup>Cs and <sup>137</sup>Cs in seawater revealed the initial arrival of the Fukushima signal by ocean current transport at a location 1,500 km west of British Columbia, Canada, in June 2012, about 1.3 y after the accident. By June 2013, the Fukushima signal had spread onto the Canadian continental shelf, and by February 2014, it had increased to a value of 2 Bq/m<sup>3</sup> throughout the upper 150 m of the water column, resulting in an overall doubling of the fallout background from atmospheric nuclear weapons tests. Ocean circulation model estimates that are in reasonable agreement with our measured values indicate that future total levels of <sup>137</sup>Cs (Fukushima-derived plus fallout <sup>137</sup>Cs) off the North American coast will likely attain maximum values in the 3–5 Bq/m<sup>3</sup> range by 2015–2016 before declining to levels closer to the fallout background of about 1 Bq/m<sup>3</sup> by 2021. The increase in <sup>137</sup>Cs levels in the eastern North Pacific from Fukushima inputs will probably return eastern North Pacific concentrations to the fallout levels that prevailed during the 1980s but does not represent a threat to human health or the environment.**

oceanography | tracer | Fukushima | <sup>137</sup>Cs

On March 11, 2011, an earthquake-triggered tsunami off Japan severely damaged the Fukushima Dai-ichi Nuclear Power Plants, resulting in estimated discharges of 10–30 PBq of <sup>137</sup>Cs to the atmosphere (1) and the ocean (2), with maximum levels of 68 million Bq/m<sup>3</sup> occurring at one ocean release site on April 6, 2011 (3). The resulting large oceanic plume of radioactivity dissipated rapidly in the energetic coastal waters off Japan under the influence of currents, tidal forces, and eddies, but a significant remnant was transported eastward (Fig. 1) by the Oyashio and Kuroshio current systems (4). The initial progress of the Fukushima radioactivity plume across the central Pacific was observed by Aoyama and colleagues (5) from seawater measurements of <sup>134</sup>Cs and <sup>137</sup>Cs. Ocean circulation models (6–8) predicted that the transport of waterborne contamination from Fukushima to the eastern North Pacific would occur between 2013 and 2015. To the present time, there has been no reported systematic study of the arrival of the Fukushima radioactivity plume in the eastern North Pacific or in continental waters off North America.

Shortly after the accident, an ocean monitoring program was established to detect the arrival of Fukushima radioactivity in the eastern North Pacific and Arctic oceans. Measurements of the Cs isotopes <sup>134</sup>Cs and <sup>137</sup>Cs were conducted in 2011–2014 during four missions of the *CCGS John P. Tully* on Line P (Fig. 1), a historic series of oceanographic stations extending 1,500 km westward from British Columbia, Canada, into the interior of the North Pacific. Samples were also collected as part of a 2012 mission of the *CCGS Louis S. St. Laurent* in the Beaufort Sea (Fig. 1) to detect any inputs of Fukushima radioactivity transported from the

Pacific through the Bering Sea. The monitoring of Fukushima radioactivity is simplified by the fact that the initial <sup>134</sup>Cs/<sup>137</sup>Cs ratio in Fukushima-derived radioactivity was 1 (3). Because of its short half-life ( $t_{1/2} = 2.1$  y), any residual <sup>134</sup>Cs in atmospheric fallout from nuclear weapons testing has decayed. The detection of <sup>134</sup>Cs in seawater is therefore an unequivocal “fingerprint” indicator of contamination from Fukushima, which is the only large-scale contributor of radioactivity to the Pacific Ocean other than fallout. <sup>137</sup>Cs ( $t_{1/2} = 30$  y) concentrations can then be resolved into their Fukushima and fallout components using the initial <sup>134</sup>Cs/<sup>137</sup>Cs ratio and measurements of <sup>134</sup>Cs decay-corrected to April 6, 2011, which is the time of maximum discharge to the ocean from Fukushima (4). The <sup>134</sup>Cs/<sup>137</sup>Cs tracer pair has been previously used to track ocean currents in the North Atlantic and Arctic oceans, using Cs discharges from the Sellafield (U.K.) nuclear fuel reprocessing plant (9, 10).

The results presented in this report provide a time series for the arrival of the Fukushima radioactivity signal in the eastern North Pacific and continental waters off North America. These results are compared with ocean circulation model simulations to document the accuracy of model predictions, to infer the range of future levels of Fukushima radioactivity in the eastern North Pacific, and to constrain estimates of radiologic effects on marine organisms.

## Results

The comparison of the Fukushima radioactivity signal with the fallout background is straightforward because <sup>137</sup>Cs has been tracked quite extensively in the Pacific Ocean since the peak period of atmospheric weapons testing in the early 1960s (11, 12). Levels in the region east of Japan have decreased from 10–20 Bq/m<sup>3</sup> in 1960 to 1.5 Bq/m<sup>3</sup> on average in 2010 (13). The decrease in <sup>137</sup>Cs during this 50-y period reflects both radioactive decay of <sup>137</sup>Cs and removal from the surface layer of the ocean

## Significance

The radionuclide results in this report represent the first systematic study, to our knowledge, of the arrival of the Fukushima radioactivity signal in continental waters off North America. The present time series results are critical to an understanding of the circulation of Fukushima tracers in the eastern North Pacific and to the tuning and validation of ocean circulation models that are being used to predict the future evolution of this signal. They are also important for informing the public of the magnitude of the Fukushima radioactivity signal in North American continental waters and enabling a science-based assessment of the significance of its potential effects on human health and the environment.

Author contributions: R.M.B. designed research; W.J.W., M.R., R.N., and S.B.M. performed research; and J.N.S. wrote the paper.

The authors declare no conflict of interest.

This article is a PNAS Direct Submission.

Freely available online through the PNAS open access option.

<sup>1</sup>To whom correspondence should be addressed. Email: john.smith@df-o-mpo.gc.ca.

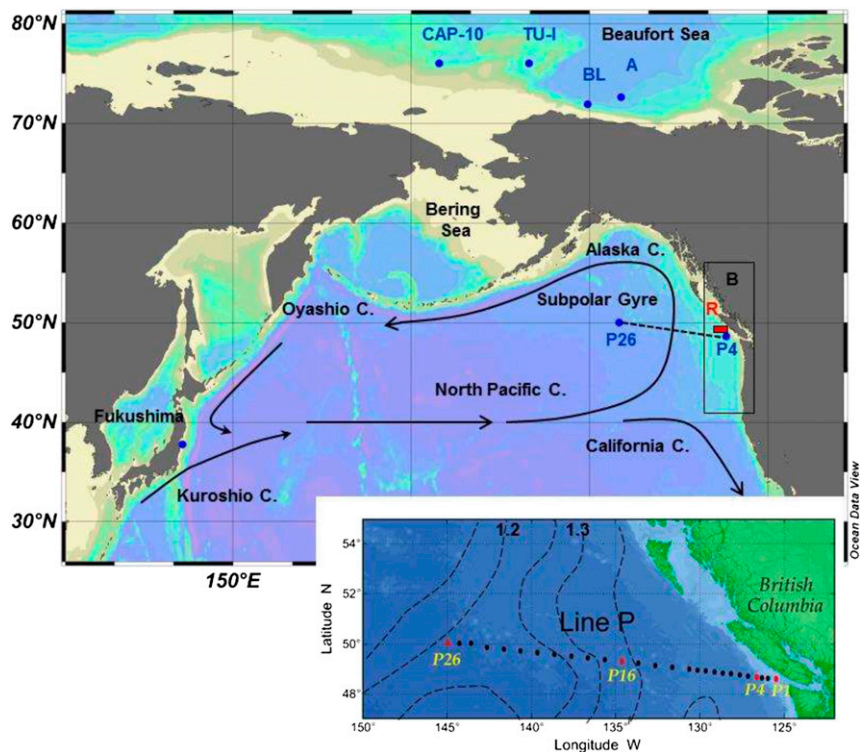


**Fig. 1.** Map showing the location of the site of the Fukushima Dai-ichi Nuclear Power Plant accident in Japan. Stations are indicated at which seawater samples were collected in 2011–2014 on Line P and in 2012 in the Beaufort Sea. Box B represents the model domain for which Fukushima-derived  $^{137}\text{Cs}$  time-series concentrations were estimated by Behrens and colleagues (6). Station R is the cross-shelf regime for which the Rossi and colleagues (7, 8) model results apply. (Inset) Sampling station locations along Line P. Dashed curves are time-averaged streamlines representing the mean dynamic height field for 2002–2012, indicating the northward geostrophic transport of the Alaska Current across Line P.

by mixing. In the present study, measurements of  $^{137}\text{Cs}$  on Line P, focusing particularly on stations P4 and P26, are intended to intercept the eastward flow of Fukushima radioactivity in the North Pacific and Alaska currents at the eastern edge of the subpolar gyre (Fig. 1). Station P4 is situated at the edge of the continental shelf at a water depth of 1,300 m and provides a sampling perspective for flow onto or adjacent to the shelf, whereas station P26, located at a depth of 4,250 m, anchors Line P offshore and is the location of a time series site for observing ocean processes.

The distributions of  $^{137}\text{Cs}$  concentrations with water depth at stations P4 and P26 for the June 2011 *CCGS John P. Tully* mission are illustrated in Fig. 2A and given in Table 1. At both stations,  $^{137}\text{Cs}$  concentrations in 2011 were 1–1.5  $\text{Bq/m}^3$  in the upper 100 m of the surface mixed layer, decreasing to values of about 0.1  $\text{Bq/m}^3$  at 1,000 m. Levels of  $^{134}\text{Cs}$  were below the detection limit of 0.13  $\text{Bq/m}^3$  in all samples, indicating that the observed  $^{137}\text{Cs}$  was entirely derived from fallout and that no detectable contamination from the Fukushima accident was present at that time. The first observations of detectable  $^{134}\text{Cs}$  on Line P were made at station P26 in June 2012 (Fig. 2A).  $^{134}\text{Cs}$  levels of 0.2–0.4  $\text{Bq/m}^3$  [decay-corrected to April 6, 2011 (4)] were measured in the upper 100 m, clearly indicating the presence of Fukushima-derived radioactivity. The Fukushima  $^{134}\text{Cs}$  signal had not yet traveled sufficiently eastward to be detectable at station P4 by June 2012. However, by June 2013,  $^{134}\text{Cs}$  was detectable in the upper 100 m at all stations sampled on Line P (Fig. 2A and B), thereby signaling the arrival of the Fukushima radioactivity plume of  $^{134}\text{Cs}$  and  $^{137}\text{Cs}$  in North American continental waters.  $^{134}\text{Cs}$  concentrations in surface water were 0.8 and 0.4  $\text{Bq/m}^3$  at stations P26 and P4, respectively, in June 2013. Because the initial  $^{134}\text{Cs}/^{137}\text{Cs}$  ratio in Fukushima-derived

radioactivity was 1 (3), the measured  $^{134}\text{Cs}$  concentration on Line P, decay-corrected to April 6, 2011, is directly equivalent to the  $^{137}\text{Cs}$  concentration discharged from Fukushima and is hereafter referred to as the Fukushima  $^{137}\text{Cs}$  concentration (Table 1). Between June 2013 and February 2014, the Fukushima-derived  $^{137}\text{Cs}$  concentration in the surface mixed layer at station P26 continued to increase to a level of about 2  $\text{Bq/m}^3$ , resulting in an increase in total  $^{137}\text{Cs}$  levels (Fukushima plus fallout  $^{137}\text{Cs}$ ) to 3.6  $\text{Bq/m}^3$ . However, only smaller or even negligible increases were observed in the 2014 Fukushima  $^{137}\text{Cs}$  signal at stations, such as station P4 (Fig. 2A), that are located proximal to the continental shelf.

The cross sectional distribution of the Fukushima  $^{137}\text{Cs}$  concentration along Line P in June 2013 is illustrated in Fig. 2B. The Fukushima  $^{137}\text{Cs}$  signal was restricted to the upper 150 m of the water column, which is the approximate depth of the winter mixed layer in the eastern North Pacific (14). The decreasing gradient in the Fukushima  $^{137}\text{Cs}$  surface mixed layer concentration (Fig. 2B) extending from station P26 to station P1 reflects the eastward circulation of Fukushima radioactivity from the ocean interior. However, most of the eastward decrease in the Fukushima  $^{137}\text{Cs}$  concentration both in 2013 and 2014 occurred in the region between station P20 and station P16 that is heavily influenced by the northward flowing Alaska Current (Fig. 1).

Line P is situated in the vicinity of the bifurcation of the North Pacific Current, where the large-scale circulation diverges into the northward-flowing Alaska Current and the southward-flowing California Current (Fig. 1). These flows are subject to pronounced variability on interannual to decadal time scales (15). Time-averaged streamlines representing the mean dynamic height field for 2002–2012 calculated from Project Argo float data ([www.medsdmm.dfo-mpo.gc.ca/isdm-gdsi/argo/canadian-products/index-eng.html](http://www.medsdmm.dfo-mpo.gc.ca/isdm-gdsi/argo/canadian-products/index-eng.html)) are illustrated in the inset for Fig. 1 (14). The mean

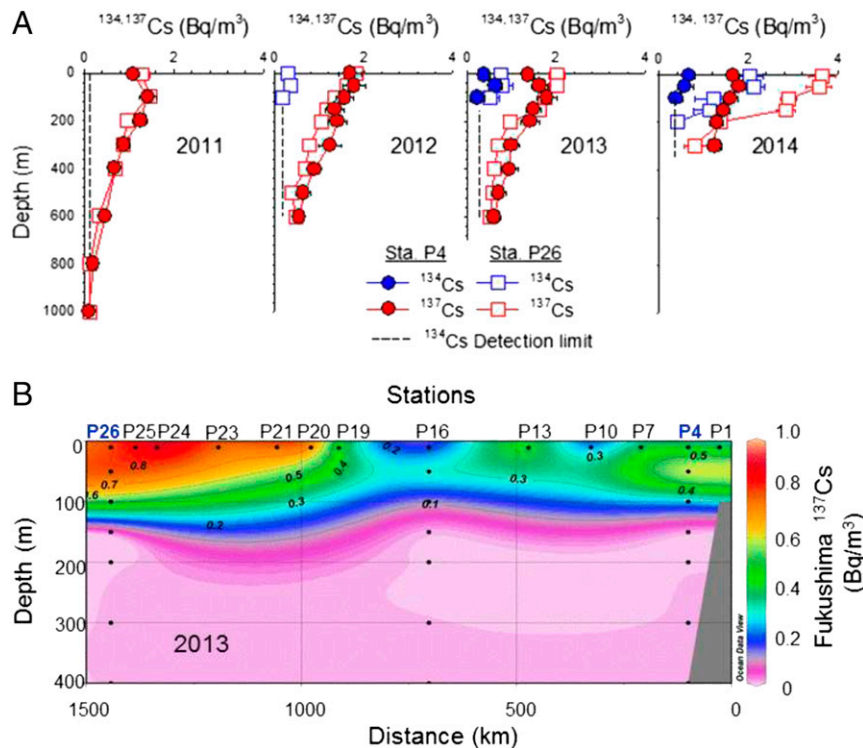


**Fig. 2.** (A) Water-depth profiles of  $^{134,137}\text{Cs}$  measured at stations P4 and P26 in June 2011, June 2012, June 2013, and February 2014 (from left to right) illustrate the arrival of  $^{134}\text{Cs}$  and  $^{137}\text{Cs}$  from the Fukushima accident on Line P. In 2011,  $^{134}\text{Cs}$  was below the detection limit (dashed line) at both stations, but was measurable (concentrations and detection limit are decay-corrected to April 6, 2011) at station P26 in 2012 and at both stations P4 and P26 in 2013 and 2014. (B) Water-depth section of Fukushima  $^{137}\text{Cs}$  concentrations (calculated from decay-corrected  $^{134}\text{Cs}$  concentrations) on Line P in June 2013 shows an eastward, decreasing  $^{137}\text{Cs}$  concentration gradient from station P26 to station P1 in the surface mixed layer that reflects  $^{137}\text{Cs}$  transport from Fukushima onto the continental shelf. Negligible Fukushima  $^{137}\text{Cs}$  had been transported below 150 m by June 2013.

streamlines are concentrated on the western part of Line P (west of station P15), which on average intercepts the northward geostrophic transport of the Alaska Current with flow speeds of 5–10 cm/s. The streamlines diverge markedly on the eastern side of Line P, which lies generally within the bifurcation zone. The flow in this region is highly variable, and mean currents are weak and difficult to define. The decreasing  $^{137}\text{Cs}$  tracer gradient in the surface mixed layer eastward along Line P (Fig. 2B) represents a transition from higher levels in the northward-flowing core of the Fukushima tracer plume to lower levels in the weaker, transitional flow field of the bifurcation zone. This slower eastward flow of the Fukushima signal onto the shelf may explain why the Fukushima  $^{137}\text{Cs}$  signal had yet to be detected by mid-2014 in Pacific coastal regions off British Columbia by a Woods Hole Oceanographic Institution crowd sourcing program ([www.ourradioactiveocean.org](http://www.ourradioactiveocean.org)). Seasonally variable winds are also a factor in the exchange of water between the open ocean and the shelf, resulting in a downwelling regime that dominates through most of the year off British Columbia (16). Downwelling tends to enhance, rather than weaken, offshore transport and likely does not contribute to the delayed transport of the Fukushima  $^{137}\text{Cs}$  signal onto the shelf along Line P.

In contrast to the North Pacific results,  $^{137}\text{Cs}$  concentrations measured in Pacific water collected in the upper 170 m of the Arctic Ocean in September 2012 were in the range (1.1–1.8 Bq/m<sup>3</sup>) associated with fallout (Table 2).  $^{134}\text{Cs}$  levels were below the detection limit (0.13 Bq/m<sup>3</sup>) at all depths at stations A, BL, CAP-10, and TU-1, located in the inflow region for Pacific water entering the Beaufort Sea (Fig. 1). These results indicate that as of September 2012, detectable Fukushima radioactivity had yet to reach the Arctic Ocean by ocean current transport through the Bering Sea. This observation is consistent with the view that

the Bering Sea is downstream of Line P in the large-scale ocean circulation pathway of the North Pacific subpolar gyre (17). The higher  $^{137}\text{Cs}$  levels (>2 Bq/m<sup>3</sup>) measured at depths below 200 m (Table 2) represent radionuclide contaminants transported into the Arctic Ocean from the North Atlantic Ocean that were discharged from European nuclear fuel reprocessing plants (18).

## Discussion

Ocean circulation models (6–8) indicate that the initial spreading of the Fukushima tracer signal was governed by the large-scale horizontal currents and mesoscale eddy fields off Japan in 2011, in conjunction with vertical turbulent mixing. These model simulations reveal a postaccident, broadening tracer patch propelled across the central North Pacific at about 40°N by the North Pacific Current (Fig. 1). The principle component of the tracer field in these simulations reaches the coastal waters of North America in several years and eventually occupies a broad region of the eastern North Pacific from Alaska to California. The Line P time series for surface water concentrations of Fukushima  $^{137}\text{Cs}$  at stations P4 and P26 is compared with the results of two model simulations (6–8) of the lateral dispersion of the Fukushima tracer plume off British Columbia in Fig. 3. Behrens and colleagues (6) predicted Fukushima  $^{137}\text{Cs}$  concentrations to first become measurable in the surface mixed layer of the area defined by Box B in Fig. 1 in 2015, 2 y after Fukushima  $^{137}\text{Cs}$  was detected at station P4. In contrast, Rossi and colleagues (7, 8) predicted the arrival of Fukushima  $^{137}\text{Cs}$  in surface water at station R, a 300-km-wide coastal band at 49°N (Fig. 1), to occur in early 2013. The model simulation reported by Rossi and colleagues (7, 8) is in good agreement with the timing of the initial detection of the Fukushima  $^{137}\text{Cs}$  signal at the nearby location of station P4 (Fig. 3). Rossi and colleagues (7) had initially



**Table 1. Time series for total <sup>137</sup>Cs and Fukushima <sup>137</sup>Cs results ( $\pm 2$  sigma uncertainties) for given water depths for stations P4 (longitude 126.67°W; latitude 48.67°N) and P26 (longitude 145.00°W; latitude 50.00°N)**

Mission and depth, m	Station P4		Station P26	
	Total <sup>137</sup> Cs, Bq/m <sup>3</sup>	Fukushima <sup>137</sup> Cs, Bq/m <sup>3</sup>	Total <sup>137</sup> Cs, Bq/m <sup>3</sup>	Fukushima <sup>137</sup> Cs, Bq/m <sup>3</sup>
<b>June 2011</b>				
5	1.09 ± 0.14	bd	1.28 ± 0.19	bd
100	1.42 ± 0.20	bd	1.46 ± 0.13	bd
200	1.25 ± 0.16	bd	0.96 ± 0.14	bd
300	0.88 ± 0.14	bd	0.86 ± 0.13	bd
400	0.68 ± 0.10	bd	0.68 ± 0.10	bd
600	0.47 ± 0.08	bd	0.34 ± 0.08	bd
800	0.20 ± 0.06	bd	0.17 ± 0.05	bd
1000	0.10 ± 0.04	bd	0.11 ± 0.05	bd
<b>June 2012</b>				
5	1.69 ± 0.25	bd	1.84 ± 0.15	0.30 ± 0.16
50	1.78 ± 0.26	bd	1.63 ± 0.14	0.36 ± 0.13
100	1.58 ± 0.20	bd	1.34 ± 0.11	0.19 ± 0.07
150	1.35 ± 0.22	bd	1.18 ± 0.15	bd
200	1.41 ± 0.22	bd	0.87 ± 0.17	bd
300	1.24 ± 0.25	bd	0.79 ± 0.11	bd
400	0.90 ± 0.12	bd	0.70 ± 0.12	bd
500	0.60 ± 0.16	bd	0.40 ± 0.09	bd
600	0.56 ± 0.07	bd	0.48 ± 0.10	bd
<b>June 2013</b>				
0	1.38 ± 0.13	0.38 ± 0.14	2.01 ± 0.18	0.76 ± 0.12
50	1.63 ± 0.18	0.64 ± 0.15	2.01 ± 0.31	0.79 ± 0.23
100	1.79 ± 0.22	0.23 ± 0.16	1.75 ± 0.14	0.53 ± 0.21
150	1.50 ± 0.16	bd	1.62 ± 0.18	bd
200	1.42 ± 0.22	bd	0.97 ± 0.13	bd
300	1.00 ± 0.19	bd	0.71 ± 0.14	bd
400	0.95 ± 0.19	bd	0.62 ± 0.17	bd
500	0.72 ± 0.16	bd	0.57 ± 0.13	bd
600	0.61 ± 0.15	bd	0.51 ± 0.15	bd
<b>February 2014</b>				
0	1.65 ± 0.14	0.66 ± 0.14	3.64 ± 0.29	2.03 ± 0.30
50	1.79 ± 0.15	0.58 ± 0.18	3.58 ± 0.28	2.11 ± 0.25
100	1.60 ± 0.16	0.38 ± 0.14	2.89 ± 0.17	1.21 ± 0.41
150	1.44 ± 0.15	bd	2.84 ± 0.20	1.12 ± 0.36
200	1.29 ± 0.15	bd	1.37 ± 0.13	0.41 ± 0.11
300	1.25 ± 0.16	bd	0.81 ± 0.26	bd

Fukushima <sup>137</sup>Cs is calculated from <sup>134</sup>Cs measurement, as outlined in the text. All data are decay-corrected to April 6, 2011. <sup>134</sup>Cs levels below the detection limit of 0.13 Bq/m<sup>3</sup> at the time of measurement are listed as bd.

predicted Fukushima <sup>137</sup>Cs concentrations to increase rapidly to a value of 27 Bq/m<sup>3</sup> at station R by 2015. However, they have recently downscaled their results by a factor of 10 (8) to levels that are in good agreement with the Line P measurements (Fig. 3). The time series of Rossi and colleagues (7, 8) for Fukushima <sup>137</sup>Cs slightly lags the measured values at the ocean interior location, station P26, and slightly leads the time series at station P4. The revised simulation of Rossi and colleagues (7, 8) indicates that a maximum Fukushima <sup>137</sup>Cs level of 2.8 Bq/m<sup>3</sup> will be attained at station R in 2015.

Estimates of the total Fukushima <sup>137</sup>Cs input into the ocean vary widely from 3.5 PBq (19) to 27 PBq (20), most of which are based on a combination of numerical analyses and direct observations. Recent estimates of the Fukushima release into the ocean of 14.5 PBq (21) and 16.2 PBq (22), based on higher-resolution simulations, tend to favor a source strength intermediate between those used in the model simulations reported by Behrens and colleagues (6) and those reported by Rossi and colleagues (7, 8). The agreement of the magnitude of the <sup>137</sup>Cs signal in the model simulations with the experimental results on Line P (Fig. 3) is consistent with the latter estimates (21, 22) of the Fukushima inputs.

The Line P data generally conform to measurements of the magnitude and timing for the eastward transport of the main Fukushima radioactivity plume by Aoyama and colleagues (5). They defined the leading edge of the Fukushima <sup>137</sup>Cs plume by the 10 Bq/m<sup>3</sup> iso-concentration front based on samples collected in the central North Pacific in 2011–2012. Their results revealed a Fukushima <sup>137</sup>Cs signal decreasing approximately exponentially with time by mixing with a time constant of 6 mo as the radioactivity plume was transported eastward across the Pacific at a speed of about 8 cm/s (5). This propagation speed is comparable to zonal geostrophic current velocities in the core of the North Pacific Current of 5–6 cm/s (15). At this rate of transport, the leading edge of the Fukushima plume would have arrived at Line P several months after the June 2013 Line P sampling mission, with a <sup>137</sup>Cs concentration reduced by mixing to a level of 1–3 Bq/m<sup>3</sup>, which is in general agreement with the range of concentrations measured at stations P4 and P26 in 2013 and 2014 (Table 1).

Public concerns have focused on the eventual magnitude of the Fukushima radioactivity signal in the ocean and the effect of this radioactivity on marine organisms. Given that the <sup>137</sup>Cs fallout background averages about 1.2 Bq/m<sup>3</sup> in surface water on

**Table 2.**  $^{137}\text{Cs}$  results ( $\pm 2$  sigma uncertainties) for water samples collected in the Arctic Ocean in September 2012

Station	Depth, m	Longitude, °W	Latitude, °N	$^{137}\text{Cs}$ , Bq/m <sup>3</sup>
BL2	5	151.773	71.388	1.16 ± 0.31
BL2	51	151.773	71.388	1.60 ± 0.38
BL2	161	151.773	71.388	1.23 ± 0.32
TU1	5	160.261	76.016	1.54 ± 0.37
TU1	72	160.261	76.016	1.56 ± 0.23
TU1	207	160.261	76.016	1.75 ± 0.24
CAP-10	6	175.292	76.018	1.49 ± 0.15
CAP-10	30	175.292	76.018	1.80 ± 0.29
CAP-10	168	175.292	76.018	1.73 ± 0.26
A	7	144.702	72.611	1.21 ± 0.16
A	51	144.702	72.611	1.06 ± 0.34
A	102	144.702	72.611	1.70 ± 0.22
A	203	144.702	72.611	4.10 ± 0.40
A	405	144.702	72.611	4.30 ± 0.42
A	608	144.702	72.611	4.00 ± 0.48
A	810	144.702	72.611	3.50 ± 0.51
A	1015	144.702	72.611	3.10 ± 0.52

$^{134}\text{Cs}$  levels were below the detection limit of 0.13 Bq/m<sup>3</sup> in all samples.

Line P, levels of Fukushima-derived  $^{137}\text{Cs}$  in February 2014 can be viewed as ranging from 170% of the fallout background at station P26 to 75% of fallout levels at station P4. Comparison with the history of atmospheric fallout in surface water in the North Pacific (inset, Fig. 3) indicates that total  $^{137}\text{Cs}$  values (Fukushima-derived plus fallout  $^{137}\text{Cs}$ ) predicted for the models of Behrens and colleagues (6) and Rossi and colleagues (7, 8) with maximum values in the 3–5 Bq/m<sup>3</sup> range would return  $^{137}\text{Cs}$  levels in continental shelf regimes in the northeast Pacific Ocean to those fallout levels that prevailed during the 1980s. On the basis of a comparison of results between stations P26 and P4 (Fig. 2 and 3), it appears that  $^{137}\text{Cs}$  levels in the interior of the Northeast Pacific may approach values greater than those on the continental shelf. However, these concentrations of  $^{137}\text{Cs}$  in the Northeast Pacific Ocean are well below Canadian guidelines for drinking water quality, for which the maximum acceptable concentration of  $^{137}\text{Cs}$  in drinking water is 10,000 Bq/m<sup>3</sup>.

The potential effect of these predicted increases in  $^{137}\text{Cs}$  seawater concentrations on marine organisms can be evaluated using the concentration factor approach used by Kryshev and colleagues (23) in the postaccident marine environment at Fukushima. Radioactive cesium in fish is excreted through osmotic pressure regulation and elimination, so it does not bioaccumulate indefinitely. Instead, the  $^{137}\text{Cs}$  concentration in fish tissue attains a steady-state value under conditions in which the  $^{137}\text{Cs}$  concentration in seawater remains constant. The  $^{137}\text{Cs}$  concentration in fish tissue can then be characterized by a concentration factor which is a dimensionless parameter defined as the  $^{137}\text{Cs}$  concentration (Bq/kg) in the fish tissue divided by the  $^{137}\text{Cs}$  concentration (Bq/kg) in ambient seawater. The recommended literature value for the concentration factor for  $^{137}\text{Cs}$  in fish of 100 (24) can be used together with the maximum projected seawater concentration for  $^{137}\text{Cs}$  of 5 Bq/m<sup>3</sup> to give a predicted  $^{137}\text{Cs}$  concentration in fish of 0.5 Bq/kg (wet weight) or 2.5 Bq/kg (dry weight). This predicted level is several times greater than the fallout background levels of  $^{137}\text{Cs}$  in fish in the North Pacific typified by the pre-Fukushima value of 1.0 Bq/kg (25) for Bluefin tuna off California. The internal radiation dose rate to fish is the product of the  $^{137}\text{Cs}$  concentration in fish and the internal dose conversion factor [ $1.8 \times 10^{-4}$  μG/h/Bq/kg (26)]. The internal radiation dose calculated using the earlier predicted  $^{137}\text{Cs}$  concentration in fish for maximum Fukushima levels in seawater yields a value of  $4.5 \times 10^{-4}$  μGy/h. ( $450 \times 10^{-12}$  Gy/h) for

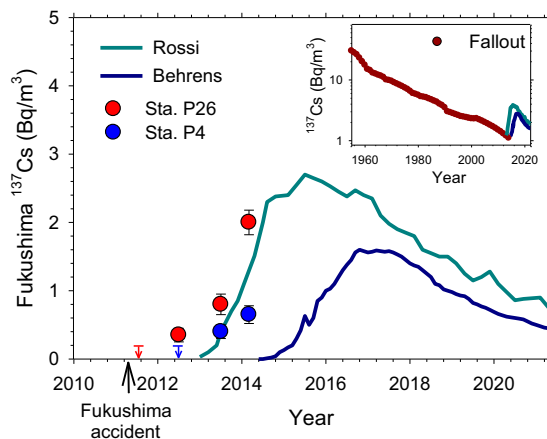


**Fig. 3.** Fukushima-derived  $^{137}\text{Cs}$  concentrations in surface water at stations P4 and P26 are illustrated for sampling dates on the bottom axis. Fukushima  $^{137}\text{Cs}$  was below the detection limit (illustrated by arrows) in 2011 but was measurable at station P26 in 2012 and measurable at both stations in 2013. Model results correspond to  $^{137}\text{Cs}$  concentrations in surface mixed layer water predicted by Behrens and colleagues (6) (blue curve) for Box B in Fig. 1 and Rossi and colleagues (7, 8) (cyan curve) for cross shelf regime R in Fig. 1. Inset shows the ocean model simulations for  $^{137}\text{Cs}$  (including an additional fallout background of 1.2 Bq/m<sup>3</sup>), which are compared with the historical record for  $^{137}\text{Cs}$  fallout levels (brown symbols) in surface waters of the North Pacific Ocean.

fish in the eastern North Pacific. This predicted exposure level is many orders of magnitude less than the baseline safe level of 420 μGy/h, below which harmful effects are not expected at either the aquatic ecosystem or the population level (27). Fisher and colleagues (28) calculated the effective radiologic dose to humans from the consumption of Bluefin tuna having levels of about 6 Bq/kg of  $^{137}\text{Cs}$  resulting from contamination from Fukushima. They noted that the dose to humans was only about 7% and 0.2% of the dose from the natural radionuclides  $^{40}\text{K}$  and  $^{210}\text{Po}$  in the fish, which is comparable to the dose commonly received from naturally occurring radionuclides in many other food items, and only a small fraction of doses from other background sources. These results indicate that future projected levels of  $^{137}\text{Cs}$  in seawater in the Northeast Pacific Ocean are well below levels posing a threat to human health or the environment.

## Methods

During oceanographic missions of the CCGS *John P. Tully* and the CCGS *Louis S. St. Laurent* in the North Pacific and Arctic oceans, respectively, large-volume ( $\approx 60$  L) water samples were collected to depths of 1,000 m and then passed through potassium cobalt ferrocyanide resin columns to selectively extract Cs isotopes from seawater (10). Column extraction efficiencies are generally greater than 96%, as determined using spiked yield tracers (10, 18), with resin columns arranged in series. The isotopes  $^{137}\text{Cs}$  and  $^{134}\text{Cs}$  were subsequently measured on the oven-dried potassium cobalt ferrocyanide resins in the laboratory, using high-purity Ge well detectors (10). All data were decay-corrected to the time, April 6, 2011, of maximum discharge from Fukushima, following Buesseler and colleagues (4). Detection limits for  $^{137}\text{Cs}$  and  $^{134}\text{Cs}$  were generally 0.10 and 0.13 Bq/m<sup>3</sup>, respectively. Detector efficiencies were measured using National Institute of Standards and Technology and National Bureau of Sciences (NBS) calibration standards (e.g., NBS 4350B river sediment) and International Atomic Energy Agency reference materials. Hydrographic results for the Line P cruises are available at [linep.waterproperties.ca](http://linep.waterproperties.ca).

**ACKNOWLEDGMENTS.** We thank the officers and crews of the CCGS *John P. Tully* and CCGS *Louis S. St. Laurent* for their assistance in sample collection and G. Forwarczna (Fisheries and Oceans Canada) and R. Kelly (University of Rhode Island) for their laboratory and field assistance. We also thank two anonymous reviewers and P. Cummins (Fisheries and Oceans Canada) for their insights and helpful comments. S.B.M. acknowledges funding support from the National Science Foundation (OCE-0926311).

1. Stohl A, et al. (2012) Xenon-133 and caesium-137 releases into the atmosphere from the Fukushima Dai-ichi nuclear power plant: Determination of the source term, atmospheric dispersion, and deposition. *Atmos Chem Phys* 12:2313–2343.
2. Charette MA, et al. (2013) Radium-based estimates of cesium isotope transport and total direct ocean discharges from the Fukushima Nuclear Power Plant accident. *Biogeosciences* 10:2159–2167.
3. Buesseler K, Aoyama M, Fukasawa M (2011) Impacts of the Fukushima nuclear power plants on marine radioactivity. *Environ Sci Technol* 45(23):9931–9935.
4. Buesseler KO, et al. (2012) Fukushima-derived radionuclides in the ocean and biota off Japan. *Proc Natl Acad Sci USA* 109(16):5984–5988.
5. Aoyama A, Uematsu U, Tsumune D, Hamajima Y (2013) Surface pathway of radioactive plume of TEPCO Fukushima NPP1 released <sup>134</sup>Cs and <sup>137</sup>Cs. *Biogeosciences Discuss* 10:265–283.
6. Behrens E, Schwarzkopf FU, Lubbecke JF, Boning CW (2012) Model simulations on the long-term dispersal of <sup>137</sup>Cs released into the Pacific Ocean off Fukushima. *Environ Res Lett* 7:034004.
7. Rossi V, et al. (2013) Multi-decadal projections of surface and interior pathways of the Fukushima cesium-137 radioactive plume. *Deep Sea Res Part I Oceanogr Res Pap* 80: 37–46.
8. Rossi V, et al. (2014) Corrigendum to “Multi-decadal projections of surface and interior pathways of the Fukushima cesium-137 radioactive plume”. *Deep Sea Res Part I Oceanogr Res Pap*, 10.1016/j.dsr.2014.08.007.
9. Livingston HD, Bowen VT, Kupferman SL (1982) Radionuclides from Windscale discharges I, Non-equilibrium tracer experiments in high latitude oceanography. *J Mar Res* 40:253–272.
10. Smith JN, Ellis KM, Jones EP (1990) Cesium-137 transport into the Arctic Ocean through Fram Strait. *J Geophys Res* 95:1693–1701.
11. Bowen VT, Noshkin VE, Livingston HD, Volchok HL (1980) Fallout radionuclides in the Pacific Ocean: Vertical and horizontal distributions, largely from GEOSECS stations. *Earth Planet Sci Lett* 49:411–434.
12. Aoyama M, et al. (2011) Cross equator transport of <sup>137</sup>Cs from North Pacific Ocean to South Pacific. *Ocean. Prog. Oceanogr.* 89:7–16.
13. Aoyama M, Hirose K (2004) Artificial radionuclides database in the Pacific Ocean: HAM database. *ScientificWorldJournal* 4:200–215.
14. Freeland HJ, Cummins PF (2005) Argo: A new tool for environmental monitoring and assessment of the world's oceans, an example from the N.E. Pacific. *Prog Ocean* 64: 31–44.
15. Cummins PF, Freeland HJ (2007) Variability of the North Pacific Current and its bifurcation. *Prog Oceanogr* 75:253–265.
16. Hickey BM, Banas NS (2003) Oceanography of the U.S. Pacific northwest coastal ocean and estuaries with application to coastal ecology. *Estuar.* 26:1010–1031.
17. Weingartner T, et al. (2005) Circulation on the north central Chukchi Sea shelf. *Deep Sea Res Part II Top Stud Oceanogr* 52:3150–3174.
18. Smith JN, et al. (2011) Iodine-129, <sup>137</sup>Cs, and CFC-11 tracer transit time distributions in the Arctic Ocean. *J Geophys Res* 116:C04024.
19. Tsumune D, Tsubono T, Aoyama M, Hirose K (2012) Distribution of oceanic <sup>137</sup>Cs from the Fukushima Dai-ichi Nuclear Power Plant simulated numerically by a regional ocean model. *J Environ Radioact* 111:100–108.
20. Bailly du Bois P, et al. (2012) Estimation of marine source-term following Fukushima Dai-ichi accident. *J Environ Radioact* 114:2–9.
21. Lai Z, et al. (2013) Initial spread of <sup>137</sup>Cs from the Fukushima Dai-ichi Nuclear Power Plant over the Japan continental shelf: A study using a high-resolution, global-coastal nested ocean model. *Biogeosci.* 10:5439–5449.
22. Rypina II, et al. (2013) Short-term dispersal of Fukushima-derived radionuclides off Japan: Modeling efforts and model-data intercomparison. *Biogeosci.* 10:4973–4990.
23. Kryshev I, Kryshev AI, Sazykina TG (2012) Dynamics of radiation exposure to marine biota in the area of the Fukushima NPP in March-May 2011. *J Environ Radioact* 114: 157–161.
24. International Atomic Energy Agency (2004) Sediment Distribution Coefficients and Concentration Factors for Radionuclides for Biota in the Marine Environment. Technical Reports Series No. 422. Available at [www-pub.iaea.org/MTCD/Publications/PDF/TRS422\\_web.pdf](http://www-pub.iaea.org/MTCD/Publications/PDF/TRS422_web.pdf). Accessed October 15, 2014.
25. Madigan DJ, Baumann Z, Fisher NS (2012) Pacific bluefin tuna transport Fukushima-derived radionuclides from Japan to California. *Proc Natl Acad Sci USA* 109(24): 9483–9486.
26. United Nations Scientific Committee on the Effects of Atomic Radiation (2011) Report of the United Nations Scientific Committee on the Effects of Atomic Radiation 2010. Fifty-Seventh Session, Includes Scientific Report: Summary of Low-Dose Radiation Effects on Health. Available at [www.unscear.org/docs/reports/2010/UNSCEAR\\_2010\\_Report\\_M.pdf](http://www.unscear.org/docs/reports/2010/UNSCEAR_2010_Report_M.pdf). Accessed October 15, 2014.
27. United Nations Scientific Committee on the Effects of Atomic Radiation (1996) Effects of Radiation on the Environment. Report to the General Assembly. Annex to Sources and Effects of Ionizing Radiation. Available at [www.unscear.org/unscear/en/publications/1996.html](http://www.unscear.org/unscear/en/publications/1996.html). Accessed October 15, 2014.
28. Fisher NS, et al. (2013) Evaluation of radiation doses and associated risk from the Fukushima nuclear accident to marine biota and human consumers of seafood. *Proc Natl Acad Sci USA* 110(26):10670–10675.